Reconciling the $X(3872)$ with the near-threshold enhancement in the $D^0\bar{D}^{*0}$ final state

C. Hanhart

Institut für Kernphysik, Forschungszentrum Jülich GmbH, D-52425 Jülich, Germany

Yu. S. Kalashnikova, A. E. Kudryavtsev, and A. V. Nefediev

Institute of Theoretical and Experimental Physics, 117218, B.Cheremushkinskaya 25, Moscow, Russia

(Received 13 April 2007; published 13 August 2007)

We investigate the enhancement in the $D^0\bar{D}^0\pi^0$ final state with the mass $M = 3875.2 \pm 0.7^{+0.3}_{-1.6} \pm 0.8$ MeV found recently by the Belle Collaboration in the $B \to KD^0\bar{D}^0\pi^0$ decay and test the possibility that this is yet another manifestation of the well-established resonance $X(3872)$. We perform a combined Flattè analysis of the data for the $D^0\bar{D}^0\pi^0$ mode and for the $\pi^+\pi^-J/\psi$ mode of the $X(3872)$. Only if the $X(3872)$ is a virtual state in the $D^0\bar{D}^{*0}$ channel do the data on the new enhancement comply with those on the $X(3872)$. In our fits, the mass distribution in the $D^0\bar{D}^{*0}$ mode exhibits a peak at 2–3 MeV above the $D^0\bar{D}^{*0}$ threshold, with a distinctive non-Breit-Wigner shape.

DOI: 10.1103/PhysRevD.76.034007 PACS numbers: 14.40.Gx, 12.39.Mk, 12.39.Pn, 13.25.Gv

I. INTRODUCTION

The $X(3872)$ state, discovered by the Belle Collaboration [1] in the B-meson decay, remains the most prominent member of the family of "homeless" charmonia, that is, those mesons which definitely contain a $\bar{c}c$ pair but do not fit the standard charmonium assignment. The state was confirmed then by the CDF [2], D0 [3], and *BABAR* [4] Collaborations. The charmonium option for the $X(3872)$ looks implausible as the state lies too high to be a $1D$ charmonium and too low to be a $2P$ one [5]. This could, in principle, mean that we simply do not understand the spectra of higher charmonia. Indeed, most of the quark model predictions consider charmonia as $c\bar{c}$ states in the quark potential model, with the potential parameters found from the description of lower charmonia, with uncertainties coming from proper treatment of relativistic effects. Another source of uncertainty is the role of open charm thresholds, a problem which is far from being resolved, though the attempts in this direction can be found in the literature—see, for example, Refs. [6,7]. In any case, it looks premature to reject the $c\bar{c}$ assignment for the $X(3872)$ on the basis of the mass only. However, further development has revealed more surprises.

The discovery mode of the $X(3872)$ is $\pi^+\pi^-J/\psi$. The observation of the $X(3872)$ in the $\gamma J/\psi$ and $\pi^+\pi^-\pi^0J/\psi$ ($\omega J/\psi$) modes [8] implies that the X has positive C-parity and the dipion in the $\pi^+\pi^-J/\psi$ mode is C-odd; that is, it originates from the ρ. Coexistence of the $\rho J/\psi$ and $\omega J/\psi$ modes points to a considerable isospin violation. Studies of the dipion mass spectrum in $X(3872) \to \pi^+\pi^-J/\psi$ decay establish that only the 1^{++} or 2^{-+} quantum number assignments are compatible with the data, while all other hypotheses are excluded by more than 3σ [9].

Both 1^{++} or 2^{-+} quantum number options for the $X(3872)$ require drastic revisions of naive quark potential models, and no alternative explanation of the 2^{-+} state in this mass region was suggested. On the other hand, it was pointed out in Refs. [10,11] that the $D\bar{D}^*$ system with 1^{++} quantum numbers can be bound by pion exchange, forming a mesonic molecule (see also Ref. [12]).[1] As confirmed by actual calculations [13], large isospin mixing due to the about 8 MeV difference between the $D^0\bar{D}^{*0}$ and D^+D^{*-} thresholds can be generated in the molecular model in quite a natural way. This model was supplied, in Ref. [14], by quark-exchange kernels responsible for the transitions $D\bar{D}^* \to \rho J/\psi, \omega J/\psi$, predicting the $\omega J/\psi$ decay mode of the $X(3872)$. Note, however, that one-pion exchange as a binding mechanism in the $D\bar{D}^*$ system should be taken with caution, as, in contrast to the NN case, here the pion can be on shell, as pointed in Ref. [15], where the ability to provide strong enough binding with one-pion exchange was questioned. For the most recent work on the implications of the nearby pion threshold, see Refs. [16,17]. For recent work for the X as a quark state, we refer to Ref. [18] and references therein.

The molecular model has received additional support with the new data on the mass of the D^0 meson [19], which yield a very weak binding

$$M_X - M(D^0\bar{D}^{*0}) = -0.6 \pm 0.6 \text{ MeV}. \tag{1}$$

In the meantime, the Belle Collaboration has reported the first observation [20] of the near-threshold enhancement in the $D^0\bar{D}^0\pi^0$ mode in the decay $B \to KD^0\bar{D}^0\pi^0$, with the branching fraction

$$\mathrm{Br}\,(B \to KD^0\bar{D}^0\pi^0) = (1.22 \pm 0.31^{+0.23}_{-0.30}) \cdot 10^{-4}. \tag{2}$$

The peak mass of the enhancement is measured to be

$$M_{\text{peak}} = 3875.2 \pm 0.7^{+0.3}_{-1.6} \pm 0.8 \text{ MeV}. \tag{3}$$

Obviously, it is tempting to relate this new state to the $X(3872)$. However, the average value of the $X(3872)$ mass

[1] An obvious shorthand notation is used here and in what follows: $D\bar{D}^* \equiv (1/\sqrt{2})(D\bar{D}^* + \bar{D}D^*)$.

is [21]

$$M_X = 3871.2 \pm 0.5 \text{ MeV}. \tag{4}$$

The central value (3) of the $D^0\bar{D}^0\pi^0$ peak mass enhancement is about 4 MeV higher than that, which obviously challenges attempts to relate this new state to the $X(3872)$.

Quite recently, the indication appeared that the Belle result [20] is likely to be confirmed. Namely, the *BABAR* Collaboration has reported the preliminary data [22] on the $B \to KD^0\bar{D}^{*0}$ decay, where the enhancement with the mass of

$$M = 3875.6 \pm 0.7^{+1.4}_{-1.5} \pm 0.8 \text{ MeV} \tag{5}$$

was found, in very good agreement with (3). *BABAR* observes the enhancement in the $D^0\bar{D}^0\pi^0$ *and* in the $D^0\bar{D}^0\gamma$ modes, which strongly supports the presence of the $D^0\bar{D}^{*0}$ intermediate state in the decay of the new X.

If the new *BABAR* data persist, and the enhancement at 3875 MeV is indeed seen in two independent experiments, the possibility should be considered seriously of the presence of two charmoniumlike states $X(3872)$ and $X(3875)$, surprisingly close to each other and to the $D^0\bar{D}^{*0}$ threshold.

However, there exists another, less exotic possibility. Namely, if the $X(3872)$ is indeed strongly coupled to the $D^0\bar{D}^{*0}$ channel, and indeed has 1^{++} quantum numbers, one could expect the existence of a near-threshold peak in the $D^0\bar{D}^{*0}$ mass distribution. In the present paper, we perform a phenomenological Flattè-like analysis of the data on the decay $B \to KD^0\bar{D}^0\pi^0$ in the near-threshold region under the assumption of the $X \to D^0\bar{D}^{*0} \to D^0\bar{D}^0\pi^0$ decay chain and 1^{++} quantum numbers for the X. The data on the $\pi^+\pi^-J/\psi$ decay modes of the $X(3872)$ are analyzed in the same framework, in order to investigate whether these data can accommodate the $X(3875)$ state as a manifestation of the $X(3872)$.

II. FLATTÈ PARAMETRIZATION

In this section, we introduce the Flattè-like parametrization of the near-threshold observables. The relevant mass range is between the thresholds for the neutral and charged D mesons. A natural generalization of the standard Flattè parametrization for the near-threshold resonance [23] of the $D^0\bar{D}^{*0}$ scattering amplitude reads

$$F(E) = -\frac{1}{2k_1}\frac{g_1k_1}{D(E)}, \tag{6}$$

with

$$D(E) = \begin{cases} E - E_f - \frac{g_1\kappa_1}{2} - \frac{g_2\kappa_2}{2} + i\frac{\Gamma(E)}{2}, & E < 0, \\ E - E_f - \frac{g_2\kappa_2}{2} + i\left(\frac{g_1k_1}{2} + \frac{\Gamma(E)}{2}\right), & 0 < E < \delta, \\ E - E_f + i\left(\frac{g_1k_1}{2} + \frac{g_2k_2}{2} + \frac{\Gamma(E)}{2}\right), & E > \delta, \end{cases} \tag{7}$$

and

$$\delta = M(D^+D^{*-}) - M(D^0\bar{D}^{*0}) = 7.6 \text{ MeV},$$
$$k_1 = \sqrt{2\mu_1 E}, \qquad \kappa_1 = \sqrt{-2\mu_1 E},$$
$$k_2 = \sqrt{2\mu_2(E-\delta)}, \qquad \kappa_2 = \sqrt{2\mu_2(\delta - E)}.$$

Here μ_1 and μ_2 are the reduced masses in the $D^0\bar{D}^{*0}$ and D^+D^{*-} channels, respectively, and the energy E is defined relative to the $D^0\bar{D}^{*0}$ threshold. In what follows, we assume isospin conservation for the coupling constants $g_1 = g_2 = g$.

The term $i\Gamma/2$ in Eq. (7) accounts for non-$D\bar{D}^*$ modes. The $X(3872)$ was observed in the $\pi^+\pi^-J/\psi$, $\pi^+\pi^-\pi^0J/\psi$, and $\gamma J/\psi$ modes, with

$$\frac{\text{Br}(X \to \pi^+\pi^-\pi^0 J/\psi)}{\text{Br}(X \to \pi^+\pi^- J/\psi)} = 1.0 \pm 0.4 \pm 0.3, \tag{8}$$

$$\frac{\text{Br}(X \to \gamma J/\psi)}{\text{Br}(X \to \pi^+\pi^- J/\psi)} = 0.14 \pm 0.05, \tag{9}$$

reported in Ref. [8]. Thus, we assume that $\Gamma(E)$ in Eq. (7) is saturated by the $\pi^+\pi^-J/\psi$ and $\pi^+\pi^-\pi^0J/\psi$ modes, and, in accordance with findings of Ref. [8], the dipion in the $\pi^+\pi^-J/\psi$ mode comes from the ρ, whereas the tripion in the $\pi^+\pi^-\pi^0J/\psi$ mode comes from the ω. The $\gamma J/\psi$ channel is neglected due to its small branching fraction (9).

The nominal thresholds for both $\rho J/\psi$ and $\omega J/\psi$ (3872 and 3879 MeV, respectively) are close to the mass range under consideration, but both the ω meson and, especially, the ρ meson have finite widths, which are large in the scale under consideration. Thus, $\Gamma(E)$ is calculated as

$$\Gamma(E) = \Gamma_{\pi^+\pi^-J/\psi}(E) + \Gamma_{\pi^+\pi^-\pi^0J/\psi}(E), \tag{10}$$

$$\Gamma_{\pi^+\pi^-J/\psi}(E) = f_\rho \int_{2m_\pi}^{M-m_{J/\psi}} \frac{dm}{2\pi} \frac{q(m)\Gamma_\rho}{(m-m_\rho)^2 + \Gamma_\rho^2/4}, \tag{11}$$

$$\Gamma_{\pi^+\pi^-\pi^0J/\psi}(E) = f_\omega \int_{3m_\pi}^{M-m_{J/\psi}} \frac{dm}{2\pi} \frac{q(m)\Gamma_\omega}{(m-m_\omega)^2 + \Gamma_\omega^2/4}, \tag{12}$$

with f_ρ and f_ω being effective couplings and

$$q(m) = \sqrt{\frac{(M^2-(m+m_{J/\psi})^2)(M^2-(m-m_{J/\psi})^2)}{4M^2}} \tag{13}$$

being the c.m. dipion/tripion momentum [$M = E + M(D^0\bar{D}^{*0})$].

Now we are in a position to write the differential rates in the Flattè approximation. These are

$$\frac{d\,\mathrm{Br}(B\to KD^0\bar{D}^{*0})}{dE}=\mathcal{B}\frac{1}{2\pi}\frac{gk_1}{|D(E)|^2}, \tag{14}$$

$$\frac{d\,\mathrm{Br}(B\to K\pi^+\pi^-J/\psi)}{dE}=\mathcal{B}\frac{1}{2\pi}\frac{\Gamma_{\pi^+\pi^-J/\psi}(E)}{|D(E)|^2}, \tag{15}$$

and

$$\frac{d\,\mathrm{Br}(B\to K\pi^+\pi^-\pi^0J/\psi)}{dE}=\mathcal{B}\frac{1}{2\pi}\frac{\Gamma_{\pi^+\pi^-\pi^0J/\psi}(E)}{|D(E)|^2}. \tag{16}$$

We assume the short-ranged dynamics of the weak $B\to K$ transition to be absorbed into the coefficient $\mathcal{B}$. Obviously, the rate (14) is defined for $E>0$ only, while the rates (15) and (16) are defined both above and below the $D^0\bar{D}^{*0}$ threshold.

The formulas (14)–(16) are valid in the zero-width approximation for the D^* mesons. In principle, one could include the finite width of the D^* mesons either analogous to Eqs. (11) and (12) or in a more sophisticated way, as there are interference effects possible in the final state, as described in Ref. [24]. However, the widths of the D^* mesons are small. Indeed, the total width of the $D^{*\pm}$ meson is measured to be 96 ± 22 keV [21]. There are no data on the D^{*0} width, but one can estimate the $D^0\pi^0$ width of the D^{*0} from the data [21] on charged $D^{*\pm}$, which gives $\Gamma(D^{*0}\to D^0\pi^0)=42$ keV. The branching fractions of D^{*0} are known [21]:

$$\mathrm{Br}\,(D^{*0}\to D^0\pi^0)=(61.9\pm 2.9)\%, \tag{17}$$

$$\mathrm{Br}\,(D^{*0}\to D^0\gamma)=(38.1\pm 2.9)\%, \tag{18}$$

so the total D^{*0} width can be estimated to be only about 68 keV. The effect of such a small width was checked to be negligible in our studies, and we assume the $D^0\bar{D}^0\pi^0$ differential rate to be

$$\frac{d\,\mathrm{Br}(B\to KD^0\bar{D}^0\pi^0)}{dE}=0.62\mathcal{B}\frac{1}{2\pi}\frac{gk_1}{|D(E)|^2}, \tag{19}$$

where the branching fraction (17) is taken into account.

Analogously, we have for the $D^0\bar{D}^0\gamma$ differential rate

$$\frac{d\,\mathrm{Br}(B\to KD^0\bar{D}^0\gamma)}{dE}=0.38\mathcal{B}\frac{1}{2\pi}\frac{gk_1}{|D(E)|^2}. \tag{20}$$

Expressions (19) and (20) neglect final-state interactions; in particular, no $D\bar{D}$ resonance within a few MeV above $D^0\bar{D}^0$ threshold is assumed to exist, and π rescattering is neglected. The latter is expected to be weak, as a consequence of chiral symmetry [17].

III. FLATTÈ ANALYSIS: PROCEDURE AND RESULTS

Let us first specify the data used in our analysis. For the $\pi^+\pi^-J/\psi$ mode, we use the data from the B-meson decay. These are the ones reported by the Belle [1] and *BABAR* [25] Collaborations. The $X(3872)$ is seen by Belle in the charged B-meson decay, with 35.7 ± 6.8 signal events and with the branching fraction [1]

$$\mathrm{Br}\,(B^+\to K^+X)\mathrm{Br}(X\to\pi^+\pi^-J/\psi)=(13.0\pm 2.9\pm 0.7)\cdot 10^{-6}. \tag{21}$$

The *BABAR* Collaboration [25] has observed the $X(3872)$ in both the charged and the neutral B-meson decays, with 61.2 ± 15.3 signal events for the charged mode and only 8.3 ± 4.5 signal events for the neutral one. The branching fraction for the charged mode was found to be

$$\mathrm{Br}\,(B^-\to K^-X)\mathrm{Br}(X\to\pi^+\pi^-J/\psi)=(10.1\pm 2.5\pm 1.0)\cdot 10^{-6}, \tag{22}$$

while the result for the neutral mode is much less certain: A 90% confidence interval was established as

$$1.34\cdot 10^{-6}<\mathrm{Br}(B^0\to K^0X)\mathrm{Br}(X\to\pi^+\pi^-J/\psi)<10.3\cdot 10^{-6}. \tag{23}$$

Because of large errors and a much smaller number of events, the $X(3872)$ peak in the neutral mode looks much less convincing than the peak in the charged mode.

A similar situation takes place for the $D^0\bar{D}^0\pi^0$ final state. The Belle data [20] include both $B^+\to K^+D^0\bar{D}^0\pi^0$ and $B^0\to K^0D^0\bar{D}^0\pi^0$ decays. There are 17.4 ± 5.2 signal events in the charged mode, with the branching fraction

$$\mathrm{Br}\,(B^+\to K^+D^0\bar{D}^0\pi^0)=(1.02\pm 0.31^{+0.21}_{-0.29})\cdot 10^{-4}, \tag{24}$$

and 6.5 ± 2.6 signal events in the neutral mode, with

$$\mathrm{Br}\,(B^0\to K^0D^0\bar{D}^0\pi^0)=(1.66\pm 0.70^{+0.32}_{-0.37})\cdot 10^{-4}. \tag{25}$$

Data on the B^+ and B^0 decays separately are presented in Ref. [26]. The $D^0\bar{D}^0\pi^0$ enhancement appears to be clearly seen in the data on charged B decays, while, again, the neutral mode displays, within the errors, a much less pronounced peak.

We conclude therefore that the data on charged and neutral B decays should be analyzed separately. The present analysis is performed for the charged mode only. Namely, with the Flattè formalism, we attempt to describe simultaneously the $\pi^+\pi^-J/\psi$ mass spectrum from the charged mode and the $D^0\bar{D}^0\pi^0$ spectrum from the B^+ mode, taken from Ref. [26].

The branching fractions (21) and (22) differ but, within the errors, are consistent with each other. In both sets of data, the fitted width of the signal is consistent with the resolution, so only the upper limits on the $X(3872)$ width were established:

$$\Gamma_{\rm tot}(\text{Belle}) < 2.3 \text{ MeV} \tag{26}$$

and

$$\Gamma_{\rm tot}(BABAR) < 4.1 \text{ MeV}, \tag{27}$$

for the Belle and *BABAR* data, respectively. In view of this discrepancy, we prefer to present two sets of fits, based on the two aforementioned sets of the $\pi^+\pi^-J/\psi$ data.

The $\pi^+\pi^-J/\psi$ data are fitted in the interval $-20 < E < 20$ MeV (as before, E is the energy relative to the $D^0\bar{D}^{*0}$ threshold), after subtraction of the full background found in the corresponding analysis. The free parameters of the fit are the short-range factor $\mathcal{B}$ and the Flattè parameters E_f, g, and f_ρ. The parameter f_ω is constrained, in accordance with Eq. (8) through the condition

$$\frac{R_{\rho J/\psi}}{R_{\omega J/\psi}} = 1, \tag{28}$$

where

$$R_{\rho J/\psi} = \int_{-20\text{ MeV}}^{20\text{ MeV}} \frac{d\,\mathrm{Br}(B\to K\pi^+\pi^-J/\psi)}{dE}dE, \tag{29}$$

$$R_{\omega J/\psi} = \int_{-20\text{ MeV}}^{20\text{ MeV}} \frac{d\,\mathrm{Br}(B\to K\pi^+\pi^-\pi^0J/\psi)}{dE}dE. \tag{30}$$

The limits of integration in Eqs. (29) and (30) are somehow arbitrary, but, as most of the support of the distributions (15) and (16) comes from within a few MeV around the $D^0\bar{D}^{*0}$ threshold, the uncertainty introduced by the limits of integration is much less than the experimental errors in Eq. (8).

The $D^0\bar{D}^0\pi^0$ data are fitted in the energy region $0 < E < 20$ MeV. Equation (19) describes the production of the $D^0\bar{D}^0\pi^0$ mode via the X resonance, while the $D\bar{D}^*$ pairs are known to be copiously produced in the $B\to K$ decay in a nonresonant way. Besides, the $D^0\bar{D}^0\pi^0$ final state could come from non-$D^0\bar{D}^{*0}$ modes such as, for example, $B\to K^*D^0\bar{D}^0$. Therefore, we are to make assumptions on the background.

The background in Refs. [20,26] is mostly combinatorial, and this part, given explicitly in the publications, was subtracted prior to the analysis. For the rest of the background, it is not possible to separate the contributions of the $D^0\bar{D}^{*0}$ and the $D^0\bar{D}^0\pi^0$ due to a limited phase space [20]. So we work under two extreme assumptions for the background. In case A, we consider the $D^0\bar{D}^0\pi^0$ background as unrelated to the $D^0\bar{D}^{*0}$ channel, while in case B, we assume that all of the $D^0\bar{D}^0\pi^0$ events come from the $D^0\bar{D}^{*0}$ mode. The background was evaluated by fitting the Belle data off peak ($25 < E < 50$ MeV). In case A, the background function is assumed to be proportional to the three-body $D^0\bar{D}^0\pi^0$ phase space $R_3 \propto E_{DD\pi}^2$, where $E_{DD\pi} = E + m_{D^{*0}} - m_{D^0} - m_{\pi^0}$. Then the total $B\to KD^0\bar{D}^0\pi^0$ differential rate is

$$\frac{d\,\mathrm{Br}^A(B\to KD^0\bar{D}^0\pi^0)}{dE} = 0.62\frac{\mathcal{B}}{2\pi}\frac{gk_1}{|D(E)|^2} + c_A E_{DD\pi}^2, \tag{31}$$

with c_A as fitting constant. In case B, the background function is proportional to the two-body $D^0\bar{D}^{*0}$ phase space $R_2 \propto k_1$ [see the definition below Eq. (7)]. Then the signal-background interference is to be taken into account:

$$\begin{aligned}\frac{d\,\mathrm{Br}^B(B\to KD^0\bar{D}^0\pi^0)}{dE} &= 0.62\frac{k_1}{2\pi}\bigg[\bigg(\mathrm{Re}\frac{\sqrt{g\mathcal{B}}}{D(E)} + c_B\cos\phi\bigg)^2 \\ &\quad + \bigg(\mathrm{Im}\frac{\sqrt{g\mathcal{B}}}{D(E)} + c_B\sin\phi\bigg)^2\bigg],\end{aligned} \tag{32}$$

with the relative phase ϕ and c_B being fitting constants.

The differential rates are translated into number-of-events distributions as follows. There are about 36 signal events in the Belle data, which corresponds to the branching fraction of about $1.3\cdot 10^{-5}$ [see Eq. (21)]. Thus the number of events per 5 MeV distribution for the $\pi^+\pi^-J/\psi$ mode is given by

$$N_{\rm Belle}^{\pi\pi J/\psi}(E) = 5\ [\mathrm{MeV}]\bigg(\frac{36}{1.3\cdot 10^{-5}}\bigg) \times \frac{d\,\mathrm{Br}(B\to K\pi^+\pi^-J/\psi)}{dE}. \tag{33}$$

For the *BABAR* data, with 61 events and the branching fraction of about $1.02\cdot 10^{-5}$ [see Eq. (22)], we have

$$N_{BABAR}^{\pi\pi J/\psi}(E) = 5\ [\mathrm{MeV}]\bigg(\frac{61}{1.02\cdot 10^{-5}}\bigg) \times \frac{d\,\mathrm{Br}(B\to K\pi^+\pi^-J/\psi)}{dE}. \tag{34}$$

As to the $D^0\bar{D}^0\pi^0$ mode, the Belle Collaboration states to have 17.4 signal events in the charged mode [20], which corresponds to the branching fraction (24) of about $1.02\cdot 10^{-4}$. The number-of-events distribution per 4.25 MeV for the $D^0\bar{D}^0\pi^0$ mode is calculated as

$$N_{A,B}^{D^0\bar{D}^0\pi^0}(E) = 4.25\ [\mathrm{MeV}]\bigg(\frac{17.4}{1.02\cdot 10^{-4}}\bigg) \times \frac{d\,\mathrm{Br}^{A,B}(B\to KD^0\bar{D}^0\pi^0)}{dE}. \tag{35}$$

The best fit to the $\pi^+\pi^-J/\psi$ data alone requires a vanishing value of the $D\bar{D}^*$ coupling constant, $g = 0$, so that such a solution cannot accommodate the $D^0\bar{D}^0\pi^0$ enhancement as a related phenomenon. To describe both $\pi^+\pi^-J/\psi$ and $D^0\bar{D}^{*0}$ modes, we are to compromise on the $\pi^+\pi^-J/\psi$ line shape.

It appears that a decent combined fit can be achieved only if the $\pi^+\pi^-J/\psi$ distribution is peaked *exactly* at the

TABLE I. The set of the Flattè parameters for the best fits to the Belle data [1,20].

Fit	g	f_ρ	f_ω	E_f, MeV	$\mathcal{B}\cdot 10^4$	ϕ
$A_{\rm Belle}$	0.3	0.0070	0.036	-11.0	11.0	$\cdots$
$B_{\rm Belle}$	0.3	0.0086	0.046	-10.9	8.9	$-144°$

TABLE II. The set of the Flattè parameters for the best fits to the *BABAR* data of Ref. [25] and the Belle data of Ref. [20].

Fit	g	f_ρ	f_ω	E_f, MeV	$\mathcal{B}\cdot 10^4$	ϕ
A_{BABAR}	0.3	0.0042	0.021	-8.8	11.4	$\cdots$
B_{BABAR}	0.3	0.0056	0.027	-8.8	8.9	$-153°$

$D^0\bar{D}^{*0}$ threshold, with the peak width (defined as the width at the peak half-height) close to the upper limits given by Eq. (26) or (27). The values of the coupling g were found to be of the order of magnitude or larger than 0.3. Finally, the fits exhibit the scaling behavior: They remain stable under the transformation

$$g\to\lambda g,\qquad E_f\to\lambda E_f,\qquad f_\rho\to\lambda f_\rho,\qquad f_\omega\to\lambda f_\omega,\qquad \mathcal{B}\to\lambda\mathcal{B}, \tag{36}$$

with tiny variations of the phase ϕ in case B.

In Tables I and II, we present the sets of the best fitting parameters—for both case A and case B and for $g=0.3$—for the Belle (Table I) and *BABAR* (Table II) data on the $\pi^+\pi^-J/\psi$ mode and for the Belle data for the $D^0\bar{D}^0\pi^0$ mode. To assess the quality of the fits, we calculate the $\pi^+\pi^-J/\psi$ distributions integrated over the 5 MeV bins, as in Refs. [1,25], and the $D^0\bar{D}^0\pi^0$ distributions integrated over the 4.25 MeV bins, as in Refs. [20,26]. The results are shown at Fig. 1 together with the experimental data.

The above-mentioned scaling behavior does not allow one to perform a proper fit with the estimate of uncertainties in the parameters found. Indeed, the parameters of the best fits found for the values of coupling constant g larger than 0.3 differ only by a few percent from the ones given by the scaling transformation (36), and the corresponding distributions are very similar to those given at Fig. 1.

As seen from the figures, acceptable fits require the $D^0\bar{D}^{*0}$ differential rate to be peaked at around 2–3 MeV above the $D^0\bar{D}^{*0}$ threshold. The scattering length in the $D^0\bar{D}^{*0}$ channel, which follows from the expression (6) of the $D^0\bar{D}^{*0}$ scattering amplitude, is given by the expression

$$a=-\frac{\sqrt{2\mu_2\delta}+2E_f/g+i\Gamma(0)/g}{(\sqrt{2\mu_2\delta}+2E_f/g)^2+\Gamma(0)^2/g^2} \tag{37}$$

and is calculated to be

$$a=\begin{cases}(-3.98-i0.46)\ \text{fm}, & \text{case }A_{\rm Belle},\\ (-3.95-i0.55)\ \text{fm}, & \text{case }B_{\rm Belle}\end{cases} \tag{38}$$

and

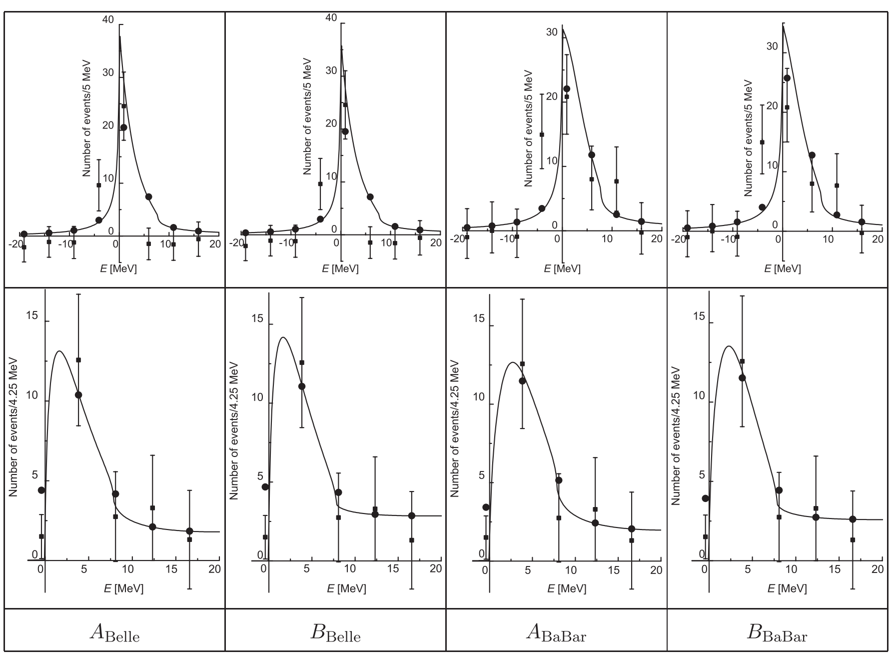

FIG. 1. Upper plots: Our fits to the differential rates for the $\pi^+\pi^-J/\psi$ channel measured by the Belle [1] and *BABAR* [25] Collaborations using prescriptions A and B [see Eqs. (31) and (32)]. Lower plots: Corresponding fits for the differential rates in the $D^0\bar{D}^0\pi^0$ channel measured by the Belle Collaboration [26]. The distributions integrated over the bins are shown in each panel as solid dots, experimental data as solid squares with error bars.

$$a = \begin{cases} (-3.10 - i0.16)\ \text{fm}, & \text{case } \mathrm{A}_{BABAR}, \\ (-3.10 - i0.22)\ \text{fm}, & \text{case } \mathrm{B}_{BABAR}. \end{cases} \tag{39}$$

The real part of the scattering length for all of the fits appears to be large and negative, and the imaginary part is much smaller. This, together with the beautiful cusp in the $\pi^+\pi^-J/\psi$ mass distribution, signals the presence of a virtual state in the $D^0\bar{D}^{*0}$ channel. The cusp scenario for the $\pi^+\pi^-J/\psi$ excitation curve in the $X(3872)$ mass range was advocated in Ref. [27]. The $X(3872)$ as a virtual $D\bar{D}^*$ state was found in the coupled-channel microscopic quark model [7].

A large scattering length explains naturally the scaling behavior of the Flattè parameters. Such a kind of scaling was described in Ref. [28] in the context of light scalar mesons properties: The scaling behavior occurs if the scattering length approximation is operative. In the case of X, the situation is more complicated, as there are two near-threshold channels, neutral and charged. Nevertheless, if it is possible to neglect the energy E in the expression (7) for the Flattè denominator $D(E)$, then, as seen from the expression (6), scaling for the $D^0\bar{D}^{*0}$ scattering amplitude indeed takes place. If the factor $\mathcal{B}$ obeys the scaling transformation, the differential rates (14)–(16) also exhibit the scaling behavior. Note that, if the energy dependence of the charged D^+D^{*-} and non-$D\bar{D}^*$ channel contributions is neglected as well, this corresponds to the scattering length approximation and neglect of the effective radius term.

IV. DISCUSSION

Our analysis shows that the large branching fraction (2) implies the X to be a virtual $D^0\bar{D}^{*0}$ state and not a bound state. We illustrate this point by calculating the rates (14) and (15) for the set of the Flattè parameters (fit C)

$$g = 0.3, \qquad E_f = -25.9\ \text{MeV}, \qquad f_\rho = 0.007, \qquad f_\omega = 0.036, \qquad \mathcal{B} = 1.32 \cdot 10^{-4}. \tag{40}$$

The values of the coupling constants coincide with those of the fit $\mathrm{A}_{\text{Belle}}$, while the parameter E_f is chosen to yield the real part of the scattering length to be equal in magnitude to the one evaluated for the given fit $\mathrm{A}_{\text{Belle}}$, but positive: $\tilde{a} = (+3.98 - i0.46)$ fm. The parameter $\mathcal{B}$ for this set yields the same value of the total branching fraction for the $\pi^+\pi^-J/\psi$ mode as the fit $\mathrm{A}_{\text{Belle}}$. The $\pi^+\pi^-J/\psi$ and $D^0\bar{D}^0\pi^0$ rates are shown in Fig. 2, together with the rates obtained for the case $\mathrm{A}_{\text{Belle}}$ (without background). The new curve (dashed line in Fig. 2) displays a very narrow peak in the $\pi^+\pi^-J/\psi$ distribution, corresponding to the $D^0\bar{D}^{*0}$ bound state, with binding energy of about 1 MeV (there is no corresponding peak in the $D^0\bar{D}^0\pi^0$ distribution as the finite width of the D^{*0} is not taken into account in our analysis). Note that the $\pi^+\pi^-J/\psi$ rates (Fig. 2) are normalized to give the branching ratio $1.3 \cdot 10^{-5}$, which re-

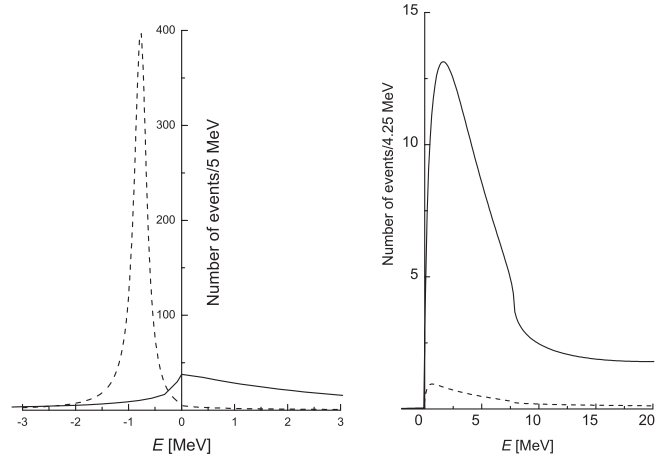

FIG. 2. The differential rates for the $\pi^+\pi^-J/\psi$ (first plot) and $D^0\bar{D}^{*0}$ (second plot) for the fits $\mathrm{A}_{\text{Belle}}$ (solid curves) and C (dashed curves).

quires the coefficient $\mathcal{B}$ to be much larger for the virtual state than for the bound state. As a result, the $D^0\bar{D}^{*0}$ rate is much smaller for the bound state, as seen from Fig. 2.

Obviously, the difference between the bound-state and virtual-state cases for the ratio

$$\frac{\mathrm{Br}(X \to D^0\bar{D}^0\pi^0)}{\mathrm{Br}(X \to \pi^+\pi^-J/\psi)} \tag{41}$$

is driven by the strength of the bound-state peak, as discussed in Ref. [29], where the scattering length approximation was used to describe the $X(3872)$. Following Ref. [29], let us write the scattering length in the $D^0\bar{D}^{*0}$ channel as

$$a = \frac{1}{\gamma_{\text{re}} + i\gamma_{\text{im}}}. \tag{42}$$

Then, in the scattering length approximation, the $\pi^+\pi^-J/\psi$ differential rate is proportional to the factor

$$\begin{aligned} &\frac{\gamma_{\text{im}}}{\gamma_{\text{re}}^2 + (k_1 + \gamma_{\text{im}})^2}, \qquad E > 0, \\ &\frac{\gamma_{\text{im}}}{(\gamma_{\text{re}} - \kappa_1)^2 + \gamma_{\text{im}}^2}, \qquad E < 0, \end{aligned} \tag{43}$$

while the $D^0\bar{D}^{*0}$ rate is proportional to

$$\frac{k_1}{\gamma_{\text{re}}^2 + (k_1 + \gamma_{\text{im}})^2}. \tag{44}$$

The line shape for the $D^0\bar{D}^{*0}$ channel does not depend on the sign of γ_{re}. The same is true for the $\pi^+\pi^-J/\psi$ line shape above the $D^0\bar{D}^{*0}$ threshold, while, below the threshold, the line shapes differ drastically: In the bound-state case, there is a narrow peak below threshold, and in the virtual-state case, a threshold cusp appears.

For $\gamma_{\text{re}} > 0$ and $\gamma_{\text{im}} \to 0$, the expression (43) becomes a δ function (see Ref. [29]):

$$\frac{\pi}{\mu_1}\gamma_{\rm re}\delta(E+\gamma_{\rm re}^2/(2\mu_1)). \tag{45}$$

Then the total rate does not depend on $\gamma_{\rm im}$, if it is small enough. This simply means that, for $\gamma_{\rm im}=0$, we have a real bound state, which is not coupled to inelastic channels. In contrast to the bound-state case, for the virtual state, the rate (43) tends to zero with $\gamma_{\rm im}\to 0$, while the $D^0\bar{D}^{*0}$ rate does not vanish in such a limit. So it is possible, by adjusting $\gamma_{\rm im}$, to obtain large values of the ratio (41).

Exactly the same situation is encountered in our fit: We need $g\gtrsim 0.3$ for the fit to be reasonable, and, in this scaling regime, as soon as we have a positive real part of the scattering length, the ratio (41) becomes small, while, with a negative real part, we get a solution compatible with the data. The large branching fraction (2) was identified in Ref. [30] as a disaster for the molecular model of the $X(3872)$. Indeed, the bound-state molecule decay into $D^0\bar{D}^0\pi^0$ is driven by the process $D^{*0}\to D^0\pi^0$, which gives the width of order $2\Gamma(D^{*0}\to D^0\pi^0)$ (up to the interference effects calculated in Ref. [24], which, for the bound-state case, cannot be neglected anymore and should be taken into account). The main decay mode of the X is $\pi^+\pi^-J/\psi$ because the phase space available is large. This is confirmed by model calculations of Ref. [14] yielding

$$\frac{\mathrm{Br}(X\to D^0\bar{D}^0\pi^0)}{\mathrm{Br}(X\to\pi^+\pi^-J/\psi)}\approx 0.08, \tag{46}$$

in strong contradiction with the data.

The estimate (46) describes the decay of an isolated bound state. However, the suppression is more moderate as, in the B decay, the continuum contribution is also to be considered. The bound-state contribution would be zero in the zero-width approximation for D^{*0}, while the $D^0\bar{D}^{*0}$ continuum contribution remains finite if the D^{*0} width is neglected. However, if the X is a bound state, the continuum contribution is not large (see Fig. 2):

$$\frac{\mathrm{Br}(X\to D^0\bar{D}^0\pi^0)}{\mathrm{Br}(X\to\pi^+\pi^-J/\psi)}\approx 0.62. \tag{47}$$

Such a small rate would remain unnoticed against the background. So, in practice, the bound state $X(3872)$ would reveal itself only as a narrow peak below threshold, with a very small rate [see Eq. (46)]. In contrast to this, we get for the virtual state

$$\frac{\mathrm{Br}(X\to D^0\bar{D}^0\pi^0)}{\mathrm{Br}(X\to\pi^+\pi^-J/\psi)}\approx 9.9. \tag{48}$$

In our analysis, the X appears to be a virtual state in the $D^0\bar{D}^{*0}$ channel. This does not contradict the assumption $g_1=g_2=g$ employed in the analysis. The latter means that the underlying strong interaction conserves isospin, and all of the isospin violation comes from the mass difference between charged and neutral $D\bar{D}^*$ thresholds. No charged partners of the X are observed, so it is reasonable to assume that the strong attractive interaction takes place in the isosinglet $D\bar{D}^*$ channel.

We do not specify the nature of this attractive force. It is known that in the one-pion-exchange model for the X, the force is attractive in the isosinglet channel and is repulsive in the isotriplet one. However, as was already mentioned, doubts were cast in Ref. [15] on the role of one-pion exchange in the $D\bar{D}^*$ binding, and it was advocated there that the X may fit the 2^3P_1 charmonium assignment if the coupling to $D\bar{D}^*$ channel is taken into account. In such a scenario, the strong binding force obviously takes place in the isosinglet channel.

We note, however, that, with the Flattè parameters found, one can make a definite statement: Whatever the nature of the $X(3872)$ is, the admixture of a compact $c\bar{c}$ state in its wave function is small. Both the large scattering length and the scaling behavior of the $D\bar{D}^*$ amplitude are consequences of the large value of the coupling constant of the state to the $D\bar{D}^*$ channel. As shown in Ref. [31], this points to a large $D\bar{D}^*$ component and a dynamical origin of the X. Although formulated for quasibound states in Ref. [31], the argument can also be generalized to virtual states. To clarify the connection between effective coupling and the nature of the state, observe that the two-point function $g(s)$ for the resonance can be written as

$$g(s)=\frac{1}{s-M^2-i\bar{\Sigma}(s)}, \tag{49}$$

where M is the physical mass of the resonance and $\bar{\Sigma}(s)=\Sigma(s)-\mathrm{Re}\Sigma(M^2)$ is the self-energy responsible for the dressing through the mesonic channels. In the near-threshold region, the momenta involved are much smaller than the inverse of the range of forces. As a result, one may neglect the s dependence of the real part of $\bar{\Sigma}$ and replace its imaginary part by the leading terms

$$g(s)\simeq\frac{1}{s-M^2+iM\sum_i g_ik_i}, \tag{50}$$

where the sum is over near-threshold channels, and the contributions of distant thresholds are absorbed into the renormalized mass M. Nonrelativistic reduction of Eq. (50) immediately yields the Flattè formula (6). Thus, the Flattè parameter E_f acquires clear physical meaning: The quantity $M(D^0\bar{D}^{*0})+E_f$ is the physical mass of the resonance, renormalized by the coupling to the decay channels.

Now, if the couplings g_i are small, the distribution for the resonance takes a standard Breit-Wigner form, and the scattering length is small. Correspondingly, the state is mostly $c\bar{c}$, with a small admixture of the $D\bar{D}^*$ component. If the couplings are large, the terms proportional to g_ik_i control the denominator in Eq. (50), the Breit-Wigner shape is severely distorted, the scattering length approximation is operative, and the mesonic component dominates the near-threshold wave function.

Formulated differently: If the couplings are large, the properties of the resonance are given mainly by the continuum contribution—which is equivalent to saying it is mostly of molecular (dynamical) nature. It should be stressed that this kind of reasoning can be used only if the resonance mass is very close to a threshold, for then the contribution of the continuum state is dominated by the unitarity cut piece which is unique and model-independent. This argument is put into more quantitative terms in Ref. [31]. It is also important to note that our analysis does not allow for any conclusion on the mechanism that leads to the molecular structure. On the level of the phenomenological parametrizations used here, a molecule formation due to t-channel exchanges and due to short-ranged s-channel forces ($c\bar{c}$-DD^* mixing) would necessarily lead to the same properties of the state, once the parameters are adjusted to the data.

V. SUMMARY

In this paper, we present a Flattè analysis of the Belle data [20] on the near-threshold enhancement in the $D^0\bar{D}^0\pi^0$ mode. We constrain the Flattè parametrization with the data on the $X(3872)$ seen in the $\pi^+\pi^-J/\psi$ and $\pi^+\pi^-\pi^0J/\psi$ modes. With such constraints, the new state can be understood as a manifestation of the well-established $X(3872)$ resonance.

We showed that the structure at 3875 MeV can only be related to the $X(3872)$ if we assume the X to be of a dynamical origin, however, not as a bound state but as a virtual state. The situation is then similar to that of nucleon-nucleon scattering in the spin-singlet channel near threshold: In contrast to the spin-triplet channel, where there exists the deuteron as a bound state, the huge scattering length in the spin-singlet channel—about 20 fm—comes from a near-threshold virtual state. The attractive interaction is just not strong enough to form a bound state in this channel as well.

The line shape in the $D^0\bar{D}^{*0}$ mode appears to differ substantially from the one extracted previously from the Belle data directly. It peaks much closer to the $D^0\bar{D}^{*0}$ threshold, though the overall description of the data looks quite reasonable within the experimental errors.

It is the $\pi^+\pi^-J/\psi$ line shape which, in our solutions, differs drastically from the one described by a simple Breit-Wigner form. We found a threshold cusp, with a width close to the limits imposed by the data analysis. While the data currently available allow for such a line shape, a considerable improvement in the experimental resolution could confirm or rule out this possibility. In the meantime, we urge the performance of an analysis of the data on the $D^0\bar{D}^0\pi^0$ final state with Flattè formulas given in Eqs. (14)–(16).

Equally important is the Flattè analysis of the $D^0\bar{D}^0\gamma$ data [22]: If the structure in the $D^0\bar{D}^0\pi^0$ is indeed due to $D^0\bar{D}^{*0}$ and is indeed related to the $X(3872)$ as a virtual state, one should observe an enhancement in $D^0\bar{D}^0\gamma$ similar to the one seen in the $D^0\bar{D}^0\pi^0$. The phase space available in this final state is larger than that in $D^0\bar{D}^0\pi^0$, so it is easier to separate the contributions of $D^0\bar{D}^{*0}$ and $D^0\bar{D}^0\gamma$ to the peak. The $D^0\bar{D}^0\gamma$ enhancement would be described with the Flattè formula (20), and, up to background and possible final-state interaction effects, the ratio of branching fractions would be

$$\frac{\mathrm{Br}(X \to D^0\bar{D}^0\pi^0)}{\mathrm{Br}(X \to D^0\bar{D}^0\gamma)} \approx 1.6. \tag{51}$$

The most interesting situation would happen if, due to an improved resolution in the $\pi^+\pi^-J/\psi$ mode, the combined Flattè analysis of the $\pi^+\pi^-J/\psi$, $D^0\bar{D}^0\pi^0$, and $D^0\bar{D}^0\gamma$ data fails to deliver a self-consistent result. Such a situation would point to the new $X(3875)$ state being completely unrelated to the $X(3872)$.

ACKNOWLEDGMENTS

We thank A. Dolgolenko for useful comments and suggestions and P. Pakhlov for illuminating discussions on various aspects of the Belle experiment. This research was supported by the Federal Agency for Atomic Energy of the Russian Federation, by Grants No. RFFI-05-02-04012-NNIOa, No. DFG-436 RUS 113/820/0-1(R), No. NSh-843.2006.2, and No. NSh-5603.2006.2, and by the Federal Programme of the Russian Ministry of Industry, Science, and Technology No. 40.052.1.1.1112. A. N. is also supported through Project No. PTDC/FIS/70843/2006-Fisica.

[1] S. K. Choi *et al.* (Belle Collaboration), Phys. Rev. Lett. **91**, 262001 (2003).
[2] D. Acosta *et al.* (CDF II Collaboration), Phys. Rev. Lett. **93**, 072001 (2004).
[3] V. M. Abazov *et al.* (D0 Collaboration), Phys. Rev. Lett. **93**, 162002 (2004).
[4] B. Aubert *et al.* (*BABAR* Collaboration), Phys. Rev. D **71**, 071103 (2005).
[5] T. Barnes and S. Godfrey, Phys. Rev. D **69**, 054008 (2004).
[6] E. Eichten, K. Gottfried, T. Kinoshita, K. D. Lane, and T. M. Yan, Phys. Rev. D **17**, 3090 (1978); **21**, 203 (1980).
[7] Yu. S. Kalashnikova, Phys. Rev. D **72**, 034010 (2005).

[8] K. Abe *et al.* (Belle Collaboration), Report No. BELLE-CONF-0540.
[9] A. Abulencia *et al.* (CDF Collaboration), Phys. Rev. Lett. **96**, 102002 (2006).
[10] M. B. Voloshin and L. B. Okun, Pis'ma Zh. Eksp. Teor. Fiz. **23**, 369 (1976) [JETP Lett. **23**, 333 (1976)].
[11] A. de Rujula, H. Georgi, and S. L. Glashow, Phys. Rev. Lett. **38**, 317 (1977).
[12] N. A. Tornqvist, Phys. Rev. Lett. **67**, 556 (1991).
[13] N. A. Tornqvist, Phys. Lett. B **590**, 209 (2004); arXiv:hep-ph/0308277.
[14] E. S. Swanson, Phys. Lett. B **588**, 189 (2004).
[15] M. Suzuki, Phys. Rev. D **72**, 114013 (2005).
[16] E. Braaten, M. Lu, and J. Lee, arXiv:hep-ph/0702128 [Phys. Rev. D (to be published)].
[17] S. Fleming, M. Kusunoki, T. Mehen, and U. van Kolck, arXiv:hep-ph/0703168 [Phys. Rev. D (to be published)].
[18] Ce Meng and Kuang-Ta Chao, Phys. Rev. D **75**, 114002 (2007).
[19] C. Cawlfield *et al.* (CLEO Collaboration), Phys. Rev. Lett. **98**, 092002 (2007).
[20] G. Gokhroo *et al.* (Belle Collaboration), Phys. Rev. Lett. **97**, 162002 (2006).
[21] W.-M. Yao *et al.* (Particle Data Group), J. Phys. G **33**, 1 (2006).
[22] P. Grenier, in Proceedings of the 42nd Rencontres de Moriond: QCD and Hadronic Interactions, http://moriond.in2p3.fr/QCD/2007/SundayAfternoon/Grenier.pdf.
[23] S. Flattè, Phys. Lett. **63B**, 224 (1976).
[24] M. B. Voloshin, Phys. Lett. B **579**, 316 (2004).
[25] B. Aubert *et al.* (*BABAR* Collaboration), Phys. Rev. D **73**, 011101 (2006).
[26] G. Majumder, in Proceedings of ICHEP2006, http://belle.kek.jp/belle/talks/ICHEP2006/Majumber.ppt.
[27] D. V. Bugg, Phys. Lett. B **598**, 8 (2004).
[28] V. Baru, J. Haidenbauer, C. Hanhart, A. Kudryavtsev, and Ulf-G. Meißner, Eur. Phys. J. A **23**, 523 (2005).
[29] E. Braaten and M. Kusunoki, Phys. Rev. D **71**, 074005 (2005).
[30] E. S. Swanson, Phys. Rep. **429**, 243 (2006).
[31] V. Baru *et al.*, Phys. Lett. B **586**, 53 (2004).